ISSN:
Print - 2277 - 0593
Online - 2315 - 7461

Journal of Natural Science, Engineering and Technology

IN SILICO IDENTIFICATION OF BIOACTIVE COMPOUNDS FROM MEDICINAL PLANTS AS POTENTIAL GLUCOKINASE INHIBITORS FOR DIABETES MANAGEMENT

***FAWIBE, O.O., UZOR, M.U., AKINYEMI, O.F., OBIWOLE, E.T., OYELAKIN, A.S., KEHINDE, I.A. AND MUSTAFA, A.A**

Department of Pure and Applied Botany, College of Biosciences, Federal University of Agriculture, Abeokuta, Nigeria
***Corresponding Author**: fawibeoo@funaab.edu.ng **Tel**: 09154120051

ABSTRACT

Diabetes, a chronic elevation in blood glucose levels, is primarily caused by the inactivation of glucokinase, a glucose sensor enzyme present in insulin-secreting pancreatic beta cells. This study investigated the inhibitory potential and proposed competitive binding mechanism of bioactive compounds from six medicinal plants: (*Mormordica charantia L., Aloe barbadensis Mill., Cinnamomum zeylanicum L., Vernonia amygdalina H., Persea americana M., and Trigonella foenum-graecum L.*) against Glucokinase active sites. Thirty (30) bioactive compounds were selected and screened together with Piragliatin (control drug). The PubChem identification number, 3D structure, and canonical SMILES of the phytocompounds and control drug were obtained using the PubChem online server. Drug likeness screening and other molecular docking analyses were carried out using web-based tools (SwissADME, AutoDock Vina, and Molinspiration). The absorption, distribution, metabolism, excretion (ADMET), and toxicity profiles of the ligands were evaluated using ADMETlab online tool. The drug-likeness screening showed that 23 of 30 bioactive compounds violated one or more of the four rules (Lipinski, Ghose, Veber, and Egan). The protein-ligand docking revealed that anthraquinone, cinnamaldehyde, coumarin, beta-amyrin, diosgenin, lutein, zeaxanthin, beta-carotene, and silymarin had higher binding energies of -8.8 kcal/mol, -7.6 kcal/mol, -8.1 kcal/mol, -7.8 kcal/mol, -8.6 kcal/mol, -7.8 kcal/mol, -7.8 kcal/mol, -8.5 kcal/mol, -7.5 kcal/mol, respectively compared with that of Piragliatin (-7.0 kcal/mol). Compounds with higher binding affinity violated at least one rule except for the non-carcinogenic anthraquinone with no drug-likeness screening violation. This study revealed anthraquinone and other lead bioactive compounds as potential antidiabetic drugs for further consideration and wet lab experimentation.

Keywords: Diabetes, Target-protein, Glucokinase, In silico studies, Molecular docking, Phytochemicals

INTRODUCTION

The escalating demand for safer, more efficient, and patient-friendly treatments is highlighted by the prevalence of diabetes and the associated difficulties. Diabetes mellitus is a global health disease. It is estimated that 463 million adults are living with diabetes, and the number is expected to rise to 700 million by 2045 (Saeedi *et al.*, 2019). This chronic metabolic disorder is characterized by persistent hyperglycemia resulting from defects in insulin secretion, insulin ac-

tion, or both, and it is classified primarily into type 1 and type 2 diabetes (American Diabetes Association, 2014). The inhibition of glucokinase (GCK), the first enzyme in glycolysis has been reported as an approach to maintaining glucose and preserving functional β-cell mass; hence, improving insulin secretion for diabetes management (Remedi and Nichols, 2023).

Current therapeutic options for diabetes treatment range from dietary modifications and to insulin therapy. However, these strategies often have limitations such as side effects, secondary failure, and the inconvenience of insulin injections (DeFronzo *et al*., 2015). Even with significant improvements in diabetes care, the condition still poses a significant threat to world health. While current treatment approaches are practical, they frequently come with adverse side effects, such as the possibility of hypoglycemia and weight gain (Davis and Johnson, 2019). Treatments like administering insulin necessitate injections, which cause difficulty and discomfort for the patients. Thus, there is a growing interest in exploring alternative antidiabetic therapies from natural resources such as medicinal plants.

Medicinal plants have been used for centuries in traditional medicine systems to treat various ailments. Traditionally, medicinal plants have been utilized to treat diabetes because of their well-known health advantages and therapeutic qualities. These plants' compounds have attracted interest as possible sources of cutting-edge antidiabetic medications with reduced adverse effects and improved patient compliance. Plants such as *Mormordica charantia*, *Aloe barbadensis* (Aloe vera), *Cinnamomum zeylanicum* (Cinnamon), *Vernonia amygdalina* (Bitter leaf), and *Persea americana* (Avocado), are traditionally known for their antidiabetic properties and have been scientifically reported to possess hypoglycemic effects (Pantidos and Boath, 2014; Ota and Ulrih, 2017).

Though antidiabetic bioactive compounds have been previously reported in the selected medicinal plants (Khare *et al*., 2016); further research is required to determine the efficacy of the bioactive compounds against the target protein and evaluate the safety and effectiveness of these compounds as potential antidiabetic drugs in comparison with existing control drug.

In the era of computational biology, bioinformatics has emerged as a powerful tool to accelerate drug discovery and understand the molecular mechanisms underlying disease pathogenesis. Switching from conventional use to efficient medications however, necessitates thorough scientific investigation and validation. Using bioinformatics techniques, particularly in silico analysis, offers a productive means of investigating and comprehending the possible connections between important diabetes-related protein targets and bioactive compounds extracted from medicinal plants. In silico techniques such as molecular docking can be used to analyze the disease-management potential of bioactive compounds from medicinal plants by predicting interactions between bioactive compounds and target proteins; thereby, contributing to the development of novel antidiabetic therapies (Kumar *et al*., 2020). Therefore, this study aimed to utilize bioinformatics tools to identify potential lead compounds from medicinal plants through in silico analysis for future antidiabetic drug development, thereby bridging traditional knowledge with modern computational biology to advance diabetes treatment.

MATERIALS AND METHODS

Ligand Selection and Preparation

Thirty (30) bioactive compounds were selected from six medicinal plants [*Mormordica charantia L.* (Bitter lemon), *Aloe barbadensis Mill.* (Aloe vera), *Cinnamomum zeylanicum L.* (Cinnamon), *Vernonia amygdalina H.* (Bitter leaf), *Persea americana M.* (Avocado), and *Trigonella foenum-graecum L.* (Fenugreek)] that have been previously reported in literature to contain active secondary metabolites capable of curing diabetes.

Kuguacin J, kuguaglycoside C, and momordicin were selected from *Mormordica charantia* (Joseph and Jini, 2013); anthraquinone, *aloesin, aloin A*, *aloe-emodin*, and barbaloin were selected from *Aloe barbadensis* miller (Radha and Laxmipriya, 2014). *Cinnamomum verum* was reported to possess cinnamaldehyde, eugenol, cinnamic acid, coumarin, and cinnamyl alcohol (Rafehi *et al.*, 2012). Vernolide, vernomygdin, vicine, quercetin, and kaempferol were reported from *Vernonia amygdalina* (Bitter leaf) (Atangwho *et al.*, 2009). Beta-sitosterol, beta-amyrin, ursolic acid, oleanolic acid were selected from *Persea americana* (Avocado) (Dreher and Davenport, 2013); 4-hydroxyisoleucine, diosgenin, fenugreekine, trigonelline, lutein, zeaxanthin, beta-carotene, and silymarin were selected from *Trigonella foenum-graecum* (Fenugreek) (Kassaian *et al.*, 2009). However, piragliatin was employed as the standard drug for comparison (Table 1). PubChem identification number (PID), the 3D structure in structure data format (SDF), and the canonical SMILES of the bioactive compounds and that of the control drugs were retrieved from PubChem web, a chemical repository server (https://pubchem.ncbi.nlm.nih.gov/compound/) (Table 1).

Protein Selection and Preparation

Glucokinase (GCK) was selected as the target protein as reported by Sternisha and Miller (2019); and its three-dimensional (3D) crystallographic structure of the target protein was downloaded from the Research Collaboratory of Structural Bioinformatics (RCSB) protein databank (www.rcsb.org) (Berman *et al.*, 2000).

In preparation for molecular docking, co-crystallized ligands and water molecules were detached and removed from the 3D structure of GCK; whereas, hydrogen was added and Gasteiger-Huckel charges was assigned?? using UCSF-Chimera (version 1.13.1) as reported by Pettersen *et al.* (2004). After these modifications, the protein structure was subjected to an energy minimization process to optimize it for molecular docking studies. The refined protein structure was thereafter preserved in the PDB file format for further analysis (Figure 1).

Table 1: Library of selected bioactive compounds with potential antidiabetic properties and their canonical smiles

S/N	Name of Compounds	ID	Canonical Smile
0	Piraglatin	10432339	CS(=O)(=O)C1=C(C=C(C=C1)C(CC2CCC(=O)C2)C(=O)NC3=NC=CN=C3)Cl
1	Anthraquinone	6780	C1=CC=C2C(=C1)C(=O)C3=CC=CC=C3C2=O
2	Aloesin	160190	CC1=CC(=CC(C2=C1C(=O)C=C(O2)CC(=O)O)C3C(C(C(C(O3)CO)O)O)O)O
3	Vicine	135413566	C(C1C(C(C(C(O1)OC2=C(N=C(NC2=O)N)N)O)O)O)O
4	Kuguacin J	25243357	CC(CC=CC(=C)C)C1CCC2(C1(CCC3(C2C(C=C4C3CCC(C4(C)C)O)OC5C(C(C(O5)CO)O)O)O)C=O)C)C
5	Kuguaglycoside C	101447827	CC(CC=CC(=C)C)C1CCC2(C1(CCC3(C2C(C=C4C3CCC(C4(C)C)O)OC5C(C(C(O5)CO)O)O)O)C=O)C)C
6	Cinnamaldehyde	637511	C1=CC=C(C=C1)C=CC=O
7	Eugenol	3314	COC1=C(C=CC=C1)CC=C)O
8	Cinnamic acid	444539	C1=CC=C(C=C1)C=CC(=O)O
9	Coumarin	323	C1=CC=C2C(=C1)C=CC(=O)O2
10	4-Hydroxyisoleucine	2773624	CC(C(O)O)C(C(=O)O)N
11	Diosgenin	99474	CC1CCC2(C(C3C(O2)CC4C3(CCC5C4CC=C6C5(CCC(C6)O)C)C)C)OC1
12	Fenugreekine	444170	C1=CC(=NC(=C1)C(=O)N)C2C(C(C(O2)COP(=O)(O)OP(=O)(O)OCC3C(C(C(O3)N4C=NC5=C(N=CN=C54)N)O)O)O)O
13	Trigonelline	5570	C[N+]1=CC=CC(=C1)C(=O)[O-]
14	Vernolide	5281508	CC(=C)C(=O)OC1CC23C(O2)CCC(=CC4C1C(=C)C(=O)O4)COC3O
15	Vernomygdin	5281509	CC(C)C(=O)OC1CC23C(O2)CCC(=CC4C1C(=C)C(=O)O4)COC3O
16	Quercetin	5280343	C1=CC(=C(C=C1C2=C(C(=O)C3=C(C=C(C=C3O2)O)O)O)O)O
17	Kaempferol	5280863	C1=CC(=CC=C1C2=C(C(=O)C3=C(C=C(C=C3O2)O)O)O)O
18	Lutein	5281243	CC1=C(C(CC(CC1O)(C)C)C=CC(=CC=CC=CC=CC=CC=CC(C)C=CC2C(=CC(CC2(C)C)O)C)C)C
19	Zeaxanthin	5280899	CC1=C(C(CC(C1O)(C)C)C=CC(=CC=CC=CC=CC=CC(C)C=CC2=C(CC(CC2(C)C)O)C)C)C
20	Beta-carotene	5280489	CC1=C(C(CCC1)(C)C)C=CC(=CC=CC=CC=CC=CC(C)C=CC2=C(CCCC2(C)C)C)C
21	Momordicin	57518366	CC1CCC2(CCC3(C4(CCC5C(C(=O)CCC5(C4C=CC3(C2C1C)O)C)(C)C)C)C)COC
22	Aloin A	12305761	C1=CC2=C(C(=C1O)C(=O)C3=C(C2C4C(C(C(O4)CO)O)O)O)C=C(C=C3O)CO
23	Aloe-emodin	10207	C1=CC2=C(C(=C1O)C(=O)C3=C(C2=O)C=C(C=C3O)CO
24	Barbaloin	44144322	C1=CC2=C(C(=C1O)C(=O)C3=C(C2C4C(C(C(O4)CO)O)O)O)C=C(C=C3O)CO
25	Cinnamyl Alcohol	5315892	C1=CC=C(C=C1)C=CCO
26	Silymarin	5213	COC1=C(C=CC(=C1)C2C(OC3=C(O2)C=C(C=C3)C4C(C(=O)C5=C(C=C(C=C5O4)O)O)O)CO)O
27	Beta-amyrin	73145	CC1(CCC2(CCC3(C(=CCC4C3(CCC5C4(CCC(C5(C)O)O)C)O)C2C1)C)C)C
28	Beta-Sitosterol	222284	CCC(CCC(C)C1CCC2C1(CCC3C2CC=C4C3(CCC(C4)O)C)C(C)C
29	Ursolic acid	64945	CC1CCC2(CCC3(C(=CCC4C3(CCC5C4(CCC(C5(C)C)O)C)C)C2C1C)C)C(=O)O
30	Oleanolic acid	10494	CC1(CCC2(CCC3(C(=CCC4C3(CCC5C4(CCC(C5(C)O)C)O)C)C2C1)C)C(=O)O)C

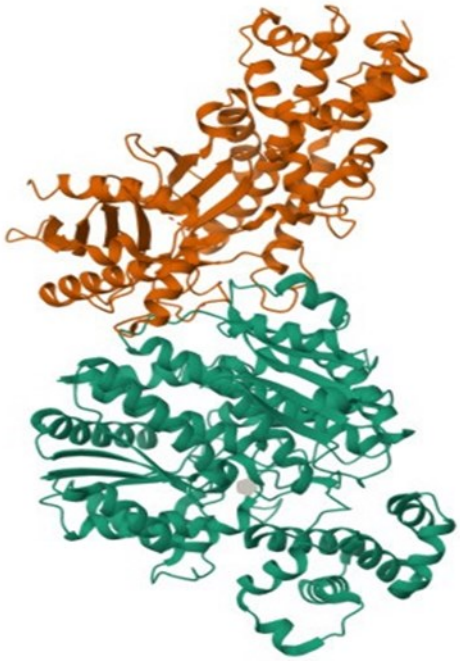

Figure 1: Structure of the protein Glucokinase (GCK) **(**Adopted from protein data bank**).**

Drug-likeness screening

The drug-likeness evaluation of thirty (30) bioactive compounds and a control drug was carried out through SwissADME web service (http://swissadme.ch/) using the canonical SMILES notation of each compound. The bioactive compounds and the control drug were subjected to four main drug likeness rules (Lipinski, Ghose, Veber, and Egan) to determine compounds with potential drug attributes. All thirty compounds, in addition with the control drug were subjected to molecular docking analysis with Glucokinase (GCK) to determine their potential interactions and affinities.

Ligand Optimization and Molecular Docking

Molecular docking of the ligands and the target protein was executed using Python-prescripted PyRx software. The three-dimensional configurations of the ligands were sequentially introduced into PyRx's integrated Open Babel tool (version 0.8), where they were energetically refined to their minimum energetic state using the Merck Molecular Force Field (MMFF94). The Ligands were then converted to AutoDock ligand format (PDBQT) for docking purposes. The molecular docking interactions between the prepared ligands and the glucokinase protein receptor were conducted via AutoDock Vina. The docking simulations were governed by a specified grid box, centering at coordinates X: 225.9940, Y: 171.7456, Z: 293.2357 with dimensions of X: 80.7873 Å, Y: 65.8779 Å, Z: 65.6821 Å to encapsulate the active site of the protein. A blind docking approach was adopted, ensuring unbiased binding site predictions with an exhaustiveness parameter set to 8 to ensure thorough sampling.

The binding affinities were derived for each ligand-protein complex and expressed in kcal/mol. The PyRx was also used to convert the docked structures from PDBQT format back to PDB format, and the files were archived for analysis and detailed structural visualization.

Molecular Interaction Analysis

The ligands and target protein were analyzed to form protein-ligand complexes using the PyMOL© molecular visualization system (version 2.4, 2010, Schrödinger LLC). The complexes were saved in PDB format and thereafter uploaded on two web -based platforms: the protein-ligand Interaction profiler (https://projects.biotec.tudresden.de/plip-web/plip) and proteins plus (https://proteins.plus) for detailed molecular interactions analyses within the complexes.

Prediction of bioactivity

The assessment of the ligands' bioactivity scores for various functionalities which included GPCR ligand, ion channel modulator, nuclear receptor ligand, kinase inhibitor, protease inhibitor, and enzyme inhibitor was conducted through the Molinspiration web service (accessible at https://www.molinspiration.com). Compounds with bioactivity scores above 0 were classified as active; scores ranging from -5.0 to 0 indicated moderate activity; and compounds with scores below -5.0 were deemed inactive.

Pharmacokinetics properties prediction

ADMETlab online tool (https://admetmesh.scbdd.com/service/evaluation/cal) was used to determine the absorption, distribution, metabolism, excretion, and toxicity (ADMET) characteristics of the ligands obtained from the molecular docking, and the results were used to predict the pharmacokinetic properties of the ligands.

RESULTS

Drug likeness screening

The drug-likeness screening result shows that twenty-three (23) out of the thirty bioactive compounds violated one or more of the four rules (Lipinski, Ghose, Veber, and Egan); however, seven (anthraquinone, eugenol, vernolide, vernomygdin, quercetin, kaemferol, aloe-emodin) successfully conformed to all of the established drug likeness rules (Table 2).

The molecular weights of all the seven (7) bioactive compounds that conformed to the drug-likeness screening rules and that of the control drug were less than 500 daltons and considered as good druggability attributes (Table 2).

Table 2: Screening result of the bioactive compounds and the control drugs using the SwissADME online tool

S/N	Molecule	Formula	MW	XLogP	TPSA	Lipinski #violations	Ghose #violations	Veber #violations	Egan #violations	Bioavailability Score
1	Piragliatin	$C_{19}H_{20}ClN_3O_4S$	421.90	1.21	114.47	0	0	0	0	0.55
2	Anthraquinone	$C_{14}H_8O_2$	208.21	3.39	34.14	0	0	0	0	0.55
3	Aloesin	$C_{19}H_{22}O9$	394.37	-1.28	157.66	0	1	1	1	0.55
4	Vicine	$C_{10}H_{16}N_4O_7$	304.26	-3.72	197.17	2	1	1	1	0.17
5	Kuguacin J	$C_{30}H_{46}O3$	454.68	6.42	57.53	1	3	0	1	0.55
6	Kuguaglycoside C	$C_{36}H_{56}O_8$	616.83	4.83	136.68	1	3	0	1	0.55
7	Cinnamaldehyde	C_9H_8O	132.16	1.9	17.07	0	2	0	0	0.55
8	Eugenol	$C_{10}H_{12}O_2$	164.2	2.27	29.46	0	0	0	0	0.55
9	Cinnamic acid	$C_9H_8O_2$	148.16	2.13	37.3	0	2	0	0	0.85
10	Coumarin	$C_9H_6O_2$	146.14	1.39	30.21	0	2	0	0	0.55
11	4-Hydroxyisoleucine	$C_6H_{13}NO_3$	147.17	-2.82	83.55	0	3	0	0	0.55
12	Diosgenin	$C_{27}H_{42}O_3$	414.62	5.67	38.69	1	2	0	0	0.55
13	Fenugreekine	$C_{21}H_{27}N_7O_{14}P_2$	663.43	-5.92	346.89	3	4	2	1	0.11
14	Trigonelline	$C_7H_7NO_2$	137.14	0.51	44.01	0	4	0	0	0.55
15	Vernolide	$C_{19}H_{22}O_7$	362.37	0.93	94.59	0	0	0	0	0.55
16	Vernomygdin	$C_{19}H_{24}O_7$	364.39	1.01	94.59	0	0	0	0	0.55
17	Quercetin	$C_{15}H_{10}O_7$	302.24	1.54	131.36	0	0	0	0	0.55
18	Kaempferol	$C_{15}H_{10}O_6$	286.24	1.9	111.13	0	0	0	0	0.55
19	Lutein	$C_{40}H_{56}O_2$	568.87	11.01	40.46	2	4	0	1	0.17
20	Zeaxanthin	$C_{40}H_{56}O_2$	568.87	10.91	40.46	2	4	0	1	0.17
21	Beta-carotene	$C_{40}H_{56}$	536.87	13.54	0	2	4	0	1	0.17
22	Momordicin	$C_{31}H_{50}O_3$	470.73	6.67	46.53	1	3	0	1	0. 55
23	Aloin A	$C_{21}H_{22}O_9$	418.39	-0.12	167.91	1	1	1	1	0.55
24	Aloe-emodin	$C_{15}H_{10}O_5$	270.24	1.82	94.83	0	0	0	0	0.55
25	Barbaloin	$C_{21}H_{22}O_9$	418.39	-0.12	167.91	1	1	1	1	0.55
26	Cinnamyl Alcohol	$C_9H_{10}O$	134.18	1.95	20.23	0	1	0	0	0.55
27	Silymarin	$C_{25}H_{22}O_{10}$	482.44	1.9	155.14	0	1	1	1	0.55
28	Beta-amyrin	$C_{30}H_{50}O$	462.72	9.15	20.23	1	3	0	1	0.55
29	Beta-Sitosterol	$C_{29}H_{50}O$	414.71	9.34	20.23	1	3	0	1	0.55
30	Ursolic acid	$C_{30}H_{48}O_3$	456.7	7.34	57.53	1	3	0	1	0.85
31	Oleanolic acid	$C_{30}H_{48}O_3$	456.7	7.49	57.53	1	3	0	1	0.85

MW: Molecular Weight; XLogP: Molecular Lipophilicity Potential; TPSA: Topological Polar Surface Area

Molecular docking and interaction between the ligands and Glucokinase

The study evaluated the binding efficiency, electrostatic energy, hydrophobic, and hydrogen bond interaction between the compounds and Glucokinase (GCK). Among the thirty bioactive compounds, nine (9) bioactive compounds had higher binding energy with GCK than the control drug Piragliatin. These compounds included: Anthraquinone, cinnamaldehyde, coumarin, beta-amyrin, diosgenin, lutein, zeaxanthin, beta-carotene, and silymarin (Table 3). Notably, anthraquinone present in Aloe barbadensis had higher binding energy (-8.8 kcal/mol) to GCK than the control drug (-7.5 kcal/mol) among others, without any violation of the drug-likeness rules (Table 3).

Cinnamaldehyde and coumarin found in *Cinnamomum verum* also had higher binding energies of -7.6 and -8.1 kcal/mol, respectively (Table 3). Beta-amyrin in *Persea americana* also had a binding energy of -7.8 kcal/mol. Diosgenin, lutein, zeaxanthin, beta-carotene, and silymarin are present in *Trigonella foenum-graecum*, bound to the active site of GCK with energies of -8.6, -7.8, -7.8, and -7.8 kcal/mol, respectively. These were considered higher than that of the control drug (Table 3).

The binding configurations of the bioactive compounds in the GCK active site are represented in Figures 3-7. Anthraquinone established two hydrogen bonds with LYS33 and ARG525 and also exhibited hydrophobic interactions with ARG525, ALA26, and ALA521 (Figure 3). Cinnamaldehyde and coumarin formed no hydrogen bonds; however, Cinnamaldehyde established hydrophobic interactions with HIS331, VAL333, PHE363, ILE396, LEU400, VAL406, and LEU422 (Figure 4a) and also formed a π stacking interaction with PHE363. Coumarin established hydrophobic interactions with HIS331, VAL333, PHE363, ILE396, LEU400, VAL406, and LEU422 (Figure 4b). Beta-amyrin formed no hydrogen bonds but exhibited hydrophobic interactions with GLN289, LEU293, and GLU294 (Figure 5). Conversely, diosgenin formed a hydrogen bond with SER78 and hydrophobic interactions with GLN72 and PRO210 (Figure 6a). Lutein formed a hydrogen bond with ASN122 and established hydrophobic interactions with PHE115, VAL119, TYR136, ASP142, ARG143, VAL146, and PHE357 (Figure 6b). Zeaxanthin formed a hydrogen bond with LYS126 and established hydrophobic interactions with VAL119, GLN123, VAL146, ALA147, ILE340, ILE343, PHE357, and LEU364 (Figure 6c). Beta-carotene did not form any hydrogen bonds but established hydrophobic interactions with ASP45, LYS48, VAL50, LYS51, GLN304, and TYR307 (Figure 6d). Moreover, silymarin formed hydrogen bonds with GLU32, ARG215, ARG227, HIS504, and GLN524 and also established hydrophobic interactions with VAL28, LYS33, and ALA521 (Figure 6e).

The control drug, piragliatin formed hydrogen bonds with LYS33 and GLN524 and established hydrophobic interactions with VAL28 and LYS33 (Figure 7).

Table 3: Binding energies and molecular interactions of bioactive compounds in the active site protein Glucokinase (GCK)

S/N	Plant source	Molecule	Binding energy (kcal/mol)	No of hydrogen bonds formed	Residues involved in hydrogen bond formation (Å)	Residues involved in hydrophobic interaction (Å)	Residue involved in π-stacking (Å)	Halogen bonds
1	*Aloe barbadensis miller*	Anthraquinone	-8.8	2	LYS33(3.05) ARG525(2.45)	ALA26(3.83) ALA521(3.61), ARG525(3.59,3.79)	-	-
2	*Cinnamomum verum*	Cinnamalde-hyde	-7.6	-		HIS331(3.60), VAL333(3.65) PHE363(3.58), ILE396(3.88,3.78) LEU400(3.44), VAL406(3.71) LEU422(3.85),	PHE363(5.02)	-
3		Coumarin	-8.1	-		HIS331(3.61), VAL333(3.63) PHE363(3.44), ILE396(3.64,3.72) LEU400(3.57), VAL406(3.47) LEU422(3.58)	-	-
4	*Persea americana*	Beta-amyrin	-7.8	-		GLN289(3.76), LEU293(3.57) GLU294(3.45)	-	-
5	*Trigonella foenum-graecum*	Diosgenin	-8.6	1	SER78(3.61)	GLN72(3.30,3.82) PRO210(3.32,3.37)	-	-
6		Lutein	**-7.8**	**1**	ASN122(3.02)	PHE115(3.46), VAL119(3.88) TYR136(3.56,3.88), ASP142(3.58) ARG143(3.78), VAL146(3.81) PHE357(3.63,3.78,3.76,3.41,3.58)	**-**	**-**
7		Zeaxanthin	-7.8	1	LYS126(1.96)	VAL119(3.43,3.73), GLN123(3.70) VAL146(3.69,3.36), ALA147(3.62) ILE340(3.77,3.59), ILE343(3.35) PHE357(3.73,3.56,3.34), LEU364(3.50)	-	-
8		Beta-carotene	**-8.5**	**-**		ASP45(3.64) LYS48(3.57,3.75,3.70), VAL50(3.76) LYS51(3.51), GLN304(3.79) TYR307(3.67,3.61)	**-**	**-**
9		Silymarin	-7.8	7	GLU32(2.94) ARG215(2.21,2.41) ARG227(3.11,3.52) HIS504(3.05) GLN524(3.82)	VAL28(3.74) LYS33(3.62), ALA521(3.16)	-	-
10	Control drug	Piraglitatin	-7.5	2	LYS33(2.65) GLN524(2.31)	VAL28(3.67,3.38) LYS33(3.69)	-	-

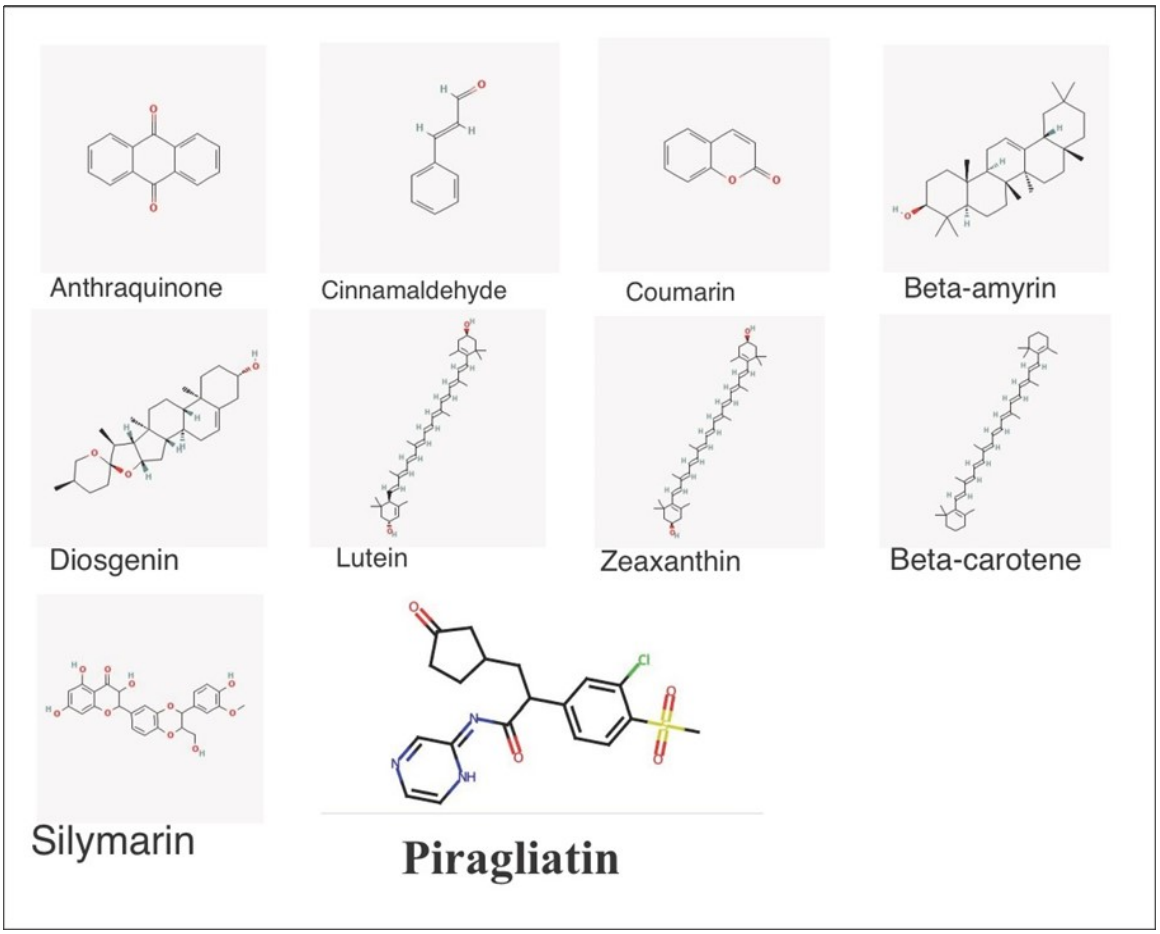

Figure 2: 2D structure of bioactive compounds and control drugs.

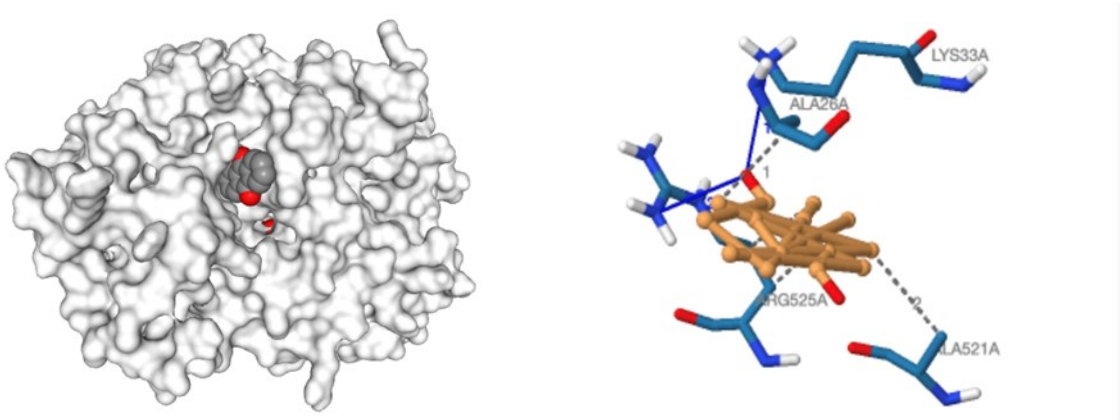

Figure 3: Interaction pattern of anthraquinone within the active site of glucokinase as obtained from molecular docking using AutoDock Vina.
Blue dashed line - Hydrogen bond; Green dotted line – Pi stacking; Grey dotted line – Hydrophobic interaction.

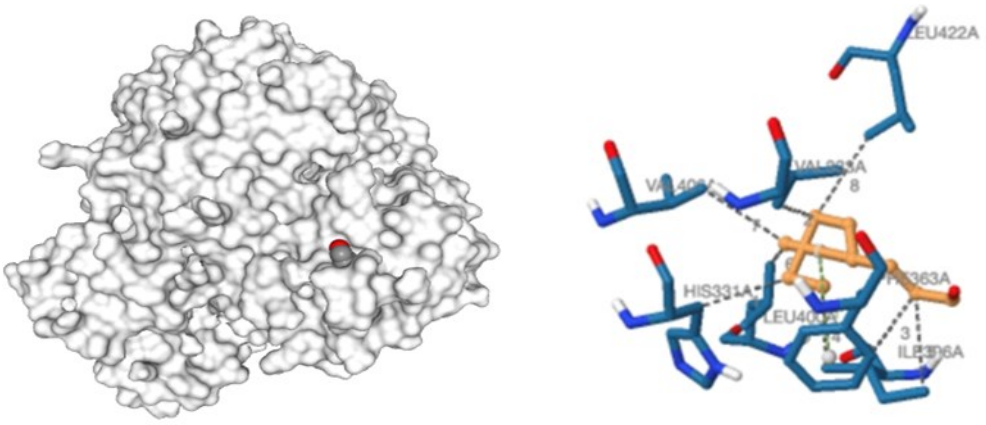

(a)

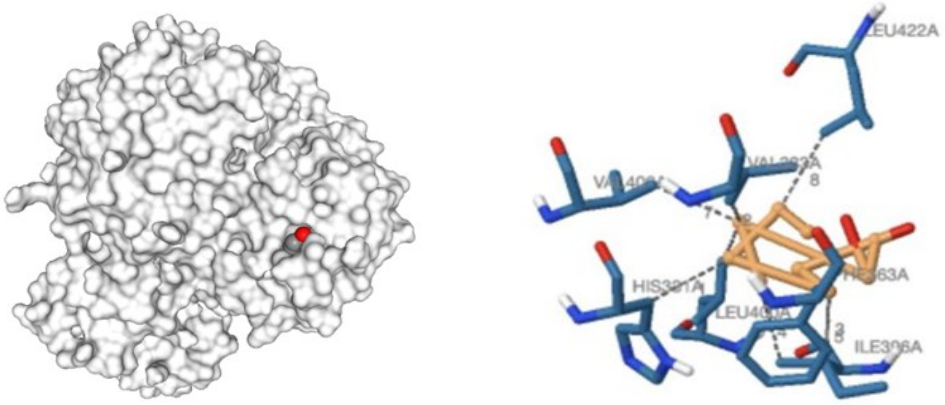

(b)

Figure 4: Molecular interactions of Cinnamaldehyde (a) and Coumarin (b) within the binding site of Glucokinase (GCK) as obtained from molecular docking using Auto-Dock Vina.
Grey dotted line – Hydrophobic interaction.

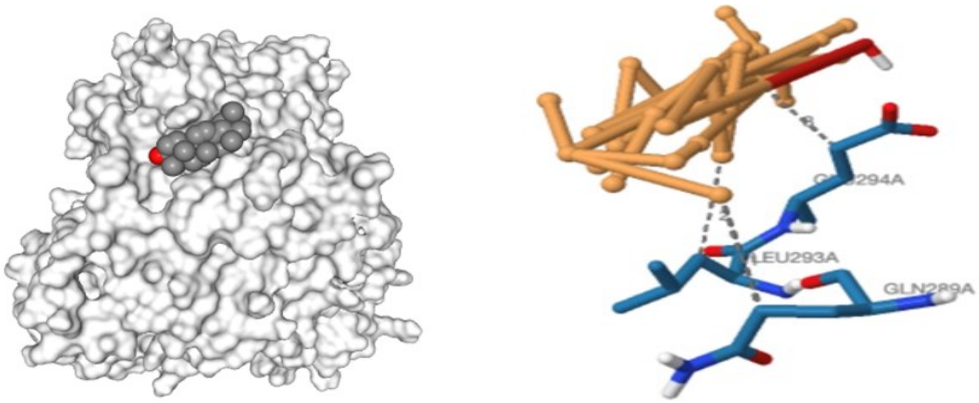

Figure 5: Binding orientation of beta-amyrin at the active site of Glucokinase (GCK) as obtained from molecular docking using AutoDock Vina.
Grey dotted line – Hydrophobic interaction.

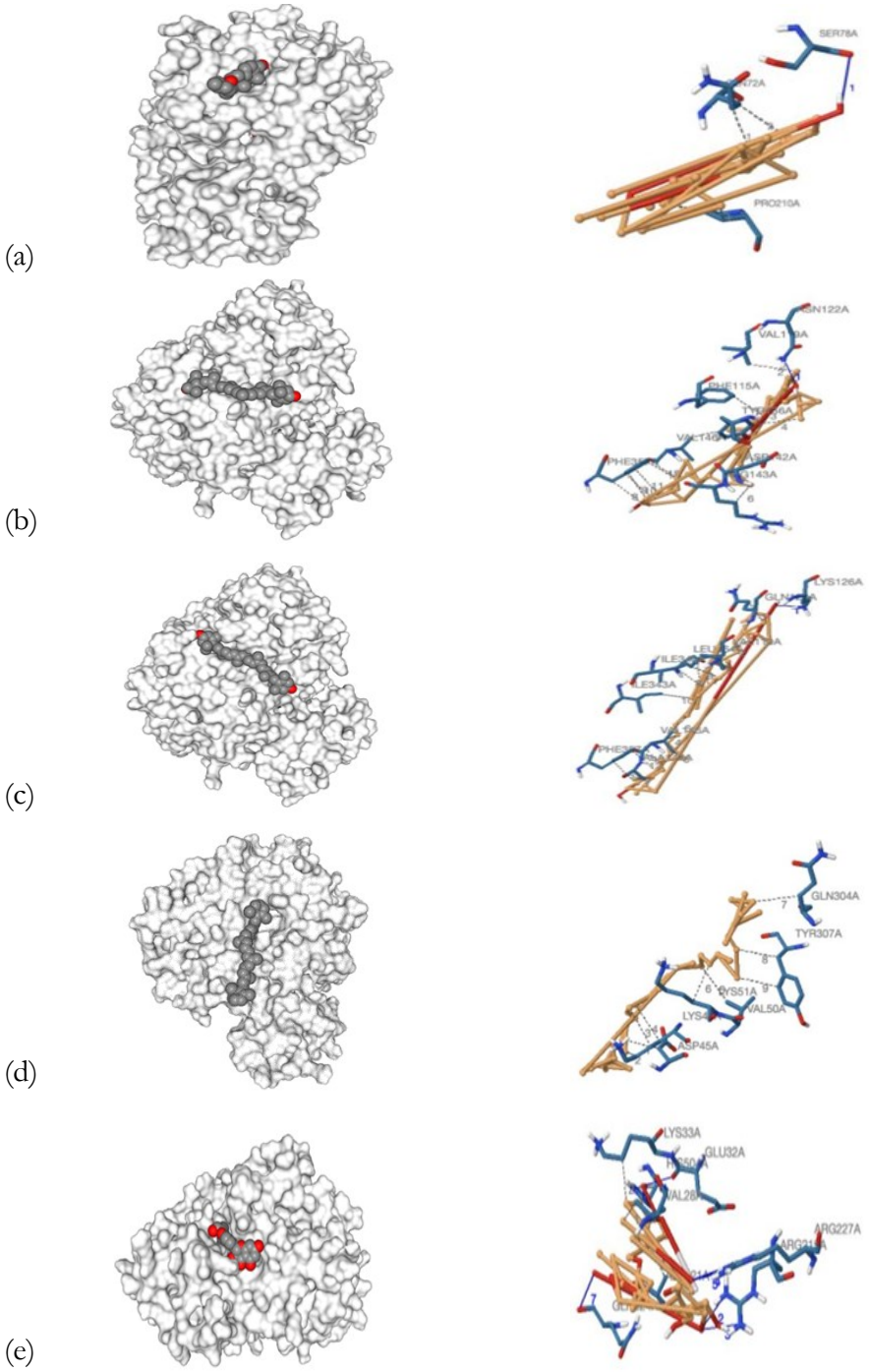

Figure 6: Binding configuration of Diosgenin (a), Lutein (b), Zeaxanthin (c), Beta-carotene (d), and Silymarin (e) in the Glucokinase active site as obtained from molecular docking using AutoDock Vina.
Blue dashed line - Hydrogen bond; Green dotted line – Pi stacking; Grey dotted line – Hydrophobic interaction.

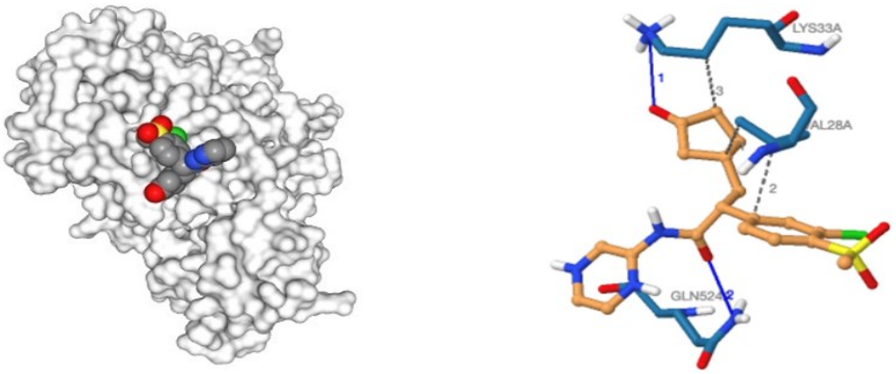

Figure 7: Binding configuration of Piragliatin within the active site of glucokinase using AutoDock.
Blue dashed line - Hydrogen bond; Grey dotted line: Hydrophobic interaction

Predicted bioactivity the ligands and control drug

All the lead ligands and the control drug had predicted values that are within the range of -5.0 to above 0 indicating that they are active or moderately active as GPCR ligands, ion channel modulators, nuclear receptor legends, kinase inhibitors, protease inhibitors, and enzyme inhibitors (Table 4). Notably, as enzyme inhibitors, anthraquinone, cinnamaldehyde, coumarin were moderately active while beta-amyrin, diosgenin, lutein, zeaxanthin, beta-carotene, and silymarin had predicted bioactivity values larger than 0.0, indicating strong activity.

Table 4: Predicted bioactivity of the ligands and the control drug

S/N	Compound name	GPCR ligand	Ion channel modulator	Kinase inhibitor	Nuclear receptor ligand	Protease inhibitor	Enzyme inhibitor
1	Anthraquinone	-0.4	-0.15	-0.30	-0.45	-0.51	-0.03
2	Cinnamaldehyde	-1.09	-0.39	-1.24	-0.96	-0.79	-0.46
3	Coumarin	-1.44	-0.86	-1.57	-1.42	-1.43	-0.58
4	Beta-amyrin	0.22	-0.05	-0.31	0.67	0.11	0.56
5	Diosgenin	0.05	-0.14	-0.57	0.58	-0.06	0.61
6	Lutein	0.03	-0.28	-0.25	0.47	-0.03	0.28
7	Zeaxanthin	-0.08	-0.36	-0.24	0.35	0.01	0.13
8	Beta-carotene	-0.04	-0.15	-0.15	0.40	-0.06	0.17
9	Silymarin	0.07	-0.05	0.01	0.16	0.02	0.23
11	Piragliatin	0.20	-0.17	-0.16	0.06	0.36	0.28

Table 5: Predicted ADMET properties of bioactive compounds and control drug

S/N. Class	Properties	Anthraquinone	Cinnamaldehyde	Coumarin	Beta-amyrin	Diosgenin	Lutein	Zeaxanthin	Beta-carotene	Silymarin	Piperlongumine
1. Absorption	**BBB**	Excellent	Poor	Excellent	Poor	Poor	Excellent	Excellent	Excellent	Excellent	Poor
	Caco-2 permeability	Excellent	Excellent	Excellent	Excellent	Excellent	Poor	Poor	Poor	Poor	Poor
	Pgp-inhibitor	Poor	Excellent	Excellent	Excellent	Excellent	Poor	Poor	Poor	Medium	Poor
	Pgp-Substrate	Excellent	Excellent	Medium	Excellent	Excellent	Poor	Poor	Medium	Excellent	Excellent
2. Distribution	**PPB**	98.453%	87.866%	87.262%	99.784%	97.743%	99.596%	99.083%	101.535%	96.657%	56.985%
	Sub-cellular localization										
3. Metabolism	**CYP450 1A2 inhibition**	Poor	Poor	Poor	Excellent	Excellent	Excellent	Excellent	Excellent	Excellent	Excellent
	CYP450 3A4 inhibition	Excellent	Excellent	Excellent	Excellent	Excellent	Excellent	Excellent	Excellent	Poor	Poor
	CYP450 3A4 substrate	Excellent	Excellent	Excellent	Medium	Medium	Poor	Poor	Poor	Medium	Poor
	CYP450 2C9 inhibition	Medium	Poor	Excellent	Excellent	Excellent	Excellent	Excellent	Excellent	Medium	Excellent
	CYP450 2C9 substrate	Medium	Medium	Medium	Medium	Excellent	Medium	Medium	Medium	Poor	Poor
	CYP450 2C19 inhibition	Medium	Excellent	Medium	Excellent	Excellent	Excellent	Excellent	Excellent	Excellent	Excellent
	CYP450 2D6 inhibition	Excellent	Excellent	Excellent	Excellent	Excellent	Medium	Medium	Excellent	Medium	Excellent
	CYP450 2D6 substrate	Excellent	Poor	Medium	Poor	Poor	Poor	Poor	Excellent	Medium	Excellent
	UGT catalyzed										
4. Toxicity	**Acute oral toxicity**	Excellent	Poor	Medium	Excellent	Poor	Excellent	Excellent	Excellent	Excellent	Medium
	hERG inhibitor	Excellent	Excellent	Excellent	Excellent	Excellent	Medium	Poor	Poor	Excellent	Poor
	Human hepatotoxicity	Excellent	Medium	Excellent	Excellent	Excellent	Excellent	Excellent	Excellent	Excellent	Poor
	Ames mutagenicity	Poor	Poor	Excellent	Excellent	Excellent	Medium	Excellent	Excellent	Medium	Excellent
	Carcinogenecity	Poor	Medium	Poor	Excellent	Excellent	Excellent	Excellent	Excellent	Medium	Excellent

BBB - blood-brain barrier, PPB - plasma protein binding, hERG - human ether-a-go-go

Pharmacokinetics prediction of bioactive compounds and the control drug

Understanding the absorption, distribution, metabolism, excretion, and toxicity (ADMET) properties of bioactive compounds is pivotal in the drug development process.

Except for cinnamaldehyde, beta-amyrin, and diosgenin, the majority of leading compounds demonstrated the potential to traverse the blood-brain barrier (BBB), a capability not shared by the control drug (Table 5). Intestinal absorption, as indicated by Caco-2 permeability, was notable for all ligands except for lutein, zeaxanthin, beta-carotene, silymarin, and the control drug piragliatin.

Anthraquinone, silymarin, and cinnamaldehyde exhibited a moderate inhibitory effect on the CYP450 2C9 enzyme, while cinnamaldehyde showed a more pronounced inhibition. Anthraquinone and cinnamaldehyde were predicted to be non mutagenic while anthraquinone and coumarin were non-carcinogenic. Other lead ligands showed some elements of carcinogenicity (Table 5).

DISCUSSION

In silico approaches predict the effectiveness of bioactive substances and their potential use as medicines. This study depicted the antidiabetic therapeutic potentials of thirty (30) bioactive compounds from six medicinal plants using in silico analysis technique.

The use of Lipinski's, Ghose's, Veber's, and Egan's guidelines for drug-likeness qualities predicted Anthraquinone, Vernolide, Vernomygdin, Quercetin, Kaempferol, Aloeemodin, Eugenol and Piragliatin (control drug) as bioactive compounds with the potential to be taken as oral drugs. This could be ascribed to their biological or pharmacological characteristics without violating the rules (Lipinski, 2001). According to Lipinski's rule of five, a bioactive compound with a molecular weight of 500 Daltons or less has good druggability and can be utilized as a drug (Lipinski *et al.*, 1997). The healing ability also depends on the drug's molecular weight. The drug-likeness results suggest that all seven bioactive substances can be employed as an oral medication, as their molecular weights are less than 500Da. Conversely, the surface area of a compound increases as the molecular weight increases beyond a specific limit, thereby reducing the penetrability of the compound.

Molecular Lipophilicity Potential (XlogP value) and Topological Polar Surface Area (TPSA) are other factors that determine drug permeability and oral bioavailability. XlogP is the logarithm of the n-octanol/water distribution coefficient that impacts membrane permeability and hydrophobic binding to macromolecules. These include the target receptor and other proteins like plasma proteins, transporters, or metabolizing enzymes. According to Lipinski's rule of five, a bioactive compound prefers hydrophilic (polar) media if its Log P value is less than 5 (LogP< 5) and prefers hydrophobic (non-polar) media if LogP value is greater than 5 (LogP > 5) (Waring, 2010). All seven (7) bioactive compounds that passed the drug-likeness screening and the control drug had LogP value that is less than five, indicating their ability to interact well in hydrophobic (non-polar) media; hence, contributing to their potential to be used as an oral drug (Brooijmans and Kuntz, 2003).

The result of this study revealed nine (9) bi-

oactive compounds out of the 30 as potent inhibitors of the GCK active site as a result of their higher binding energies than that of the control drug.

The higher binding energies of hit ligands (anthraquinone, cinnamaldehyde, coumarin, beta-amyrin, diosgenin, lutein, zeaxanthin, beta-carotene, and silymarin) than piragliatin could be attributed to their ability to form interactions in the protein-ligand complexes, which provide stability to the complexes (Hari, 2019; Usha *et al*., 2014). At the active site of Glucokinase, the hit ligands possibly competed with glucose, with their structures allowing them to form similar interactions with key amino acid residues, thereby preventing glucose from binding effectively. These probably hinder the ability of Glucokinase to convert glucose to glucose-6-phosphate, a key step in glucose metabolism, and potentially lower blood sugar levels.

Notably, anthraquinone derived from *Aloe barbadensis* had the highest binding energy of -8.8 kcal/mol among the hit ligands without violation of the drug-likeness rules. Previous study has reported anthraquinone as a valuable compound for biochemical and pharmacological studies with the potential to serve as lead structures for drug development (Malik and Muller, 2016). Based on its structure, anthraquinone was able to form hydrogen bonds, π stacking, and hydrophobic interactions with amino acid residues (LYS33, ALA521, ARG525) at the active site of Glucokinase ; hence, preventing effective binding of glucose and consequently reducing its conversion to glucose-6- phosphate.

The ability of a medicine to bind to a biological target and its therapeutic effects on living things are described by its pharmacological activity. The most popular biological targets are proteins, including enzymes, ion channels, and receptors (Rang *et al*., 2012). The results obtained from this study indicated that all the hit ligands had predicted bioactivity values that are within the range of -5.0 to above 0, indicating that they are moderately or actively binding to GPCR and nuclear receptor ligands, ion channel modulation, kinase inhibition, protease inhibition, and enzyme activity inhibition.

The ADMET properties of bioactive compounds include their capacity to bind to their target proteins and stay there for an extended amount of time to exert their therapeutic effects (Daoud *et al*., 2021; Cao *et al*., 2012). There are variations in the ADMET characteristics of the hit ligands. Lutein, Zeaxanthin, and beta-carotene were P-glycoprotein substrates. P-glycoprotein is one of the ATP binding cassette (ABC) proteins that are involved in releasing chemicals from the cell, preventing them from bioaccumulating, and evoking their reaction. Moreover, with a plasma protein binding (PPB) value of less than 90%, cinnamaldehyde and coumarin have a high therapeutic index as PPB influences the oral bioavailability of a drug.

Carcinogenicity is a toxicological endpoint of drugs with great concerns. Carcinogenic drugs may disrupt cellular metabolic processes in the human system (Baldrick and Jain, 2023; Belitskiy *et al*., 2020). Beta-amyrin, Diosgenin, Zeaxanthin, and Beta-carotene were predicted to contain some carcinogenic components. However, Anthraquinone, the bioactive compound with the highest binding energy, was non-carcinogenic and non-mutagenic. There is a need for pharmacophoric modeling, which can improve some of the fundamental ADMET properties of

the ligands. Also, molecular dynamic simulation and other wet-lab experiments are recommended to validate the results of this work.

CONCLUSION

The molecular docking of ligands with glucokinase revealed nine lead bioactive compounds (anthraquinone, cinnamaldehyde, coumarin, beta-amyrin, diosgenin, lutein, zeaxanthin, beta-carotene, and silymarin) with higher binding energy than Piragliatin (control drug). Among the nine lead ligands, anthraquinone was non carcinogenic and had no drug-likeness screening violation. With the variation in the lead-ligands toxicity levels, the study suggests anthraquinone and other lead ligands as promising antidiabetic candidates with therapeutic influence better than that of the control drug. Therefore, this study recommends pharmacophoric modeling, molecular dynamic simulation, and other wet-lab studies to validate this Insilico prediction.

REFERENCES

American Diabetes Association 2014. Diagnosis and classification of diabetes mellitus. *Diabetes Care, 37*(Suppl 1): 81-90.

Atangwho, I. J., Edet, E. E., Uti, D. E., Obi, A. U., and Asmawi, M. Z. 2009. Comparative hypoglycaemic and nephroprotective effects of Vernonia amygdalina and metformin in diabetic rats. *Journal of Medicinal Plants Research,* 3(6): 585-591.

Baldrick, P., and Jain, S. 2023. Carcinogenicity testing in drug development: Getting it right. *Regulatory Toxicology and Pharmacology*, 145:105522

Berman, H. M., Westbrook, J., Feng, Z., Gilliland, G., Bhat, T. N., Weissig, H., Shindyalov, I. N., Bourne, P. E. 2000. The Protein Data Bank. *Nucleic Acids Research*, 28: 235-242.

Brooijmans, N. and Kuntz, I. D. 2003. Molecular recognition and docking algorithms. *Annual Review of Biophysics and Biomolecular Structure,* 32: 335–373.

Cao, D., Wang, J., Zhou, R., Li, Y., Yu, H. and Hou, T. 2012. ADMET evaluation in drug discovery. 11. PharmacoKinetics Knowledge Base (PKKB): a comprehensive database of pharmacokinetic and toxic properties for drugs. *Journal of Chemical Information and Modeling,* 52(5): 1132-1137

Daoud, N. E., Borah, P., Deb, P. K., Venugopala, K. N., Hourani, W., Alzweiri, M., ... and Tiwari, V. 2021. ADMET Profiling in Drug Discovery and Development: Perspectives of In Silico, In Vitro and Integrated Approaches. *Current Drug Metabolism,* 22(7): 503-522.

Davis, R. and Johnson, S. (2019). Bioinformatics in drug development: Benefits and challenges. *Drug Discovery Today,* 24(6): 1125-1131.

DeFronzo, R. A., Ferrannini, E. and Groop, L. 2015. Type II diabetes mellitus. *Nature Reviews Disease Primers, 1*:15019.

Dreher, M. L., and Davenport, A. J. 2013. Hass avocado composition and potential health effects. *Critical Reviews in Food Science and Nutrition*, 53(7): 738-750.

Joseph, B., and Jini, D. 2013. Antidiabetic effects of Momordica charantia (bitter melon) and its medicinal potency. *Asian Pacific Journal of Tropical Disease*, 3(2): 93-102.

Kassaian, N., Azadbakht, L., Forghani, B., and Amini, M. 2009. Effect of fenugreek seeds on blood glucose and lipid profiles in type 2 diabetic patients. *International Journal for Vitamin and Nutrition Research,* 79 (1): 34-39.

Khare, C. P. 2016. Indian Medicinal Plants: An Illustrated Dictionary. Springer.

Kumar, B., Sharma, D., and Sharma, P., *et al.* 2020. In silico strategies for probing chlorogenic acid as a therapeutic agent for oxidative stress in Alzheimer's disease. *Journal of Bio molecular. Structure and Dynamics. 38* (4), 1007-1021.

Lipinski, C. A., Lombardo, F., Dominy, B. W., & Feeney, P. J. 1997. Experimental and computational approaches to estimate solubility and permeability in drug discovery and development settings. *Advanced Drug Delivery Reviews*, 23(1-3): 3-25.

Lipinski, C.A., Lombardo, F., Dominy, B.W. and Feeney, P.J. 2001. Experimental and computational approaches to estimate solubility and permeability in drug discovery and development settings. *Advanced Drug Delivery Reviews* 46(1-3): 3–26.

Ota, A. and Ulrih, N. P. 2017. An Overview of Herbal Products and Secondary Metabolites Used for Management of Type Two Diabetes. *Front Pharmacol,* 8: 436.

Pantidos, N. and Boath, A. 2014. Biological activity of *Aloe vera*. In Natural Remedies in the Fight Against Parasites. *IntechOpen*

Pettersen, E.F., Goddard, T.D., Huang, C.C., Couch, G.S., Greenblatt, D.M., Meng, E.C. and Ferrin, T.E. 2004. UCSF Chimera--a visualization system for exploratory research and analysis. *Journal of Computational Chemistry.* 25(13): 1605-12.

Radha, M. H. and Laxmipriya, N. P. 2014. Evaluation of biological properties and clinical effectiveness of Aloe vera: A systematic review. *Journal of Traditional and Complementary Medicine*: 5(1): 21–26

Rafehi, H., Ververis, K., and Karagiannis, T. C. 2012. Controversies surrounding the clinical potential of cinnamon for the management of diabetes. *Diabetes, Obesity and Metabolism,* 14(6): 493-499.

Rang, H. P. Dale, M. M. Ritter J. M. and Moore, P. K. 2012. "Pharmacology" 7th Edition, Churchill Livingstone, Edinburgh.

Remedi, M.S. and Nichols, C.G. 2023. Glucokinase Inhibition: A novel treatment for Diabetes? *Diabetes,* 72: 170-174.

Saeedi, P., Petersohn, I. and Salpea, P. 2019. Global and regional diabetes prevalence estimates for 2019 and projections for 2030 and 2045: Results from the International Diabetes Federation Diabetes Atlas. *Diabetes Research and Clinical Practice. 157*: 107843.

Sternisha, S.M. and Miller, B.G. 2019. Molecular and cellular regulation of human glucokinase. *Archives of Biochemistry and Biophysics.* 663:199-213.

Waring, M. J. 2010. Lipophilicity in drug discovery. *Expert Opinion on Drug Discovery*, 5 (3): 235-248.

(Manuscript received: 4th April, 2024; accepted: 20th June, 2024).